Strain Aging on the Yield Strength to Tensile Strength Ratio of UOE Pipe

J.B. Wiskel*, J. Ma, J. Valloton, D.G. Ivey and H. Henein

Department of Chemical and Materials Engineering, University of Alberta, 12th Floor, Donadeo ICE Bldg., 9211 - 116St., Edmonton, Alberta, Canada T6G 1H9.

* Corresponding author: bwiskel@ualberta.ca, 1-780-492-6178

Strain aging of microalloyed steel pipe can occur at the relatively low temperatures associated with the pipe coating process and/or during long term storage. A Box-Behnken statistical design is used to determine the significant strain aging variables that affect the longitudinal yield strength to tensile strength (Y/TS) ratio for three uncoated X70 UOE pipes. The strain aging variables examined include time, temperature, steel composition/microstructure (vis-a-vis the C/Nb ratio) and position through the pipe wall thickness. Metallographic and EBSD examinations were undertaken to determine the grain size and phase percentages of the as-received pipe steel. Both position in the pipe and the C/Nb ratio were found to have a statistically significant effect on the yield strength to tensile strength ratio.

Keywords: tensile properties; microalloyed steel; strain aging, Box-Behnken

1.0 Introduction

X70 (yield strength equal to 70 ksi or 480 MPa) steel pipe used for long distance transmission of oil or natural gas can be manufactured using spiral forming, electric resistance welding (ERW) or the UOE process [1]. Following pipe making, strain aging (i.e., a change in mechanical properties with time) of the steel can occur due to long term outdoor storage, the application of an anti-corrosion epoxy coating (typically applied at between 175°C to 255°C) and/or natural aging of the pipe over its lifetime. The change in mechanical properties associated with strain aging during the coating process may include an increase in yield strength (σ_y) and an increase in the yield strength to tensile strength ratio ((Y/TS)), a decrease in uniform elongation (UEL) and/or a change in the shape of the tensile curve. Strain aging can affect both the transverse and longitudinal properties of the pipe. This paper will focus solely on the Y/TS ratio for longitudinal samples.

The longitudinal mechanical properties of a pipe are important for pipeline designs where significant longitudinal loading/strain can arise due to ground movement (e.g., permafrost melting, unstable slopes, water crossings, etc.). Hence, an understanding of the longitudinal pipe properties and how these properties may change with strain aging is important in geotechnical strain based design of pipelines. These designs typically recommend a maximum value for the (Y/TS) ratio of the pipe material in the longitudinal direction. The (Y/TS) ratio is a measure of the strain capacity of the pipe material and is often used as a design parameter.

Factors that affect the (Y/TS) ratio during strain aging can include aging time and temperature, steel composition/microstructure and prior plastic deformation (i.e., strain history during forming). The work undertaken in this paper determines the effect of time, temperature, steel composition via the C/Nb ratio (microstructure variation), through wall thickness position (both microstructure and strain history variation) and macro location relative to the weld (strain history variation) on the (Y/TS) ratio of three (3) different uncoated X70 UOE pipes. Both the temperature and time values used in the study were selected to encompass the pipe coating process. A Box-Behnken Statistical Design (BBD) is used to design and analyze the aging tests conducted. Nonlinear (2^{nd} order)

equations are developed to quantify the effect of the statistically significant strain aging variable(s) (and/or a combination of variables) on the change in the yield strength to tensile strength ratio (Δ(Y/TS)). Metallography and electron backscattered diffraction (EBSD) are undertaken to determine the grain size and phase percentages of the as-received pipe material and are correlated with the Δ(Y/TS) changes observed during aging.

2.0 Background

An overview of the strain aging mechanism, recent literature on the strain aging response, and important aging variables, for microalloyed steel is presented. In addition, an introduction to statistical analysis techniques and, in particular, the Box-Behnken methodology is presented.

2.1 Strain Aging Mechanism

The basic mechanism for strain aging of steels is well established [2] and entails the diffusion of either free carbon or free nitrogen to dislocations and the subsequent stabilization/pinning of these dislocations. The segregation of carbon atoms to dislocations has been observed in steel with three-dimensional atom probe analysis [3-4]. The amount of free carbon and/or nitrogen (i.e., in solid solution) required for strain aging is typically < 0.01 wt% [5-6]. Strain aging of steel manifests itself primarily as an increase in yield stress (σ_y), but other mechanical properties [2,7] that can be influenced include tensile strength (UTS), the (Y/TS) ratio, uniform elongation (UEL), toughness, the work hardening rate and a return of discontinuous yielding (i.e., a change in the shape of the tensile curve).

2.2. Strain Aging Variables

A number of studies [8-15] have evaluated the effect of strain aging on the mechanical properties of microalloyed steel pipe. Variables analyzed in these studies include temperature, time, plastic strain and/or position/orientation of the test samples. Table I summarizes these studies and includes, where applicable, the grade of the steel pipe, whether the sample was taken from plate or pipe, sample orientation (circumferential (C) (pipe), transverse (T) (skelp) and longitudinal (L)), sample location in the pipe relative to

the seam weld, temperature, time and, for skelp starting material, the magnitude of artificially imposed strain. The consensus of the work (summarized in Table 1) is that both the yield stress and tensile strength increase with increasing temperature and plastic strain. The effect of through thickness position, microstructural features and the interaction between all the variables on strain aging is not as well addressed.

Table 1 – Summary of selected studies on strain aging of microalloyed steel pipe material

Ref.	Grade*	Type	Orientation	Location	Strain aging conditions
8	X80	pipe-UOE	C, L	±90	250°C, 1 h
9	X80	pipe-UOE	C, L	15, 90,180°	280°C, 5 min
10	X100	plate	T	n.a.	150-300°C, 1 h, ε_p=6%[#]
11	X100	plate	L	n.a.	120-240°C, 1 h
12	X100	plate	T	n.a.	150-250°C, 30 min, ε_p=1 - 3%
13	X65	pipe	T	n.a.	250 and 450°C
14	n.a.	pipe	n.a.	n.a	288°C, 30 min, ε_p=1.3 or 4%
15	X70	pipe-spiral	n.a.	15 cm weld	275°C, 1 h, ε_p=3 to 5%

* X refers to line pipe steel and 70, 80 or 100 refers to the yield strength in ksi

[#] ε_p is plastic strain

An equation to describe the strain aging mechanism (i.e., diffusion and interaction of carbon with dislocations) in steel has been developed [16].

$$\frac{N(t)}{N_{so}} = \frac{3}{2} \cdot \eta_o \cdot \lambda \cdot 2 \cdot \left(\frac{\pi}{2}\right)^{1/3} \cdot \left(\frac{A \cdot D}{kT}\right)^{2/3} \cdot t^{2/3} \qquad (1)$$

where *N(t)* is the number of dislocations pinned during the aging process, N_{so} is the initial dislocation density, T is the absolute temperature, t is time, η_o is the initial carbon concentration in solution, λ is the slip distance, k is the Boltzmann constant and *A* is an interaction parameter. The important variables defined by Equation (1) are temperature, time and the starting dislocation density (i.e., imposed plastic strain). These variables

correspond to the main variables studied in Table I. In addition, Equation (1) shows a dependence on the free carbon content. Though Equation (1) endeavours to describe the mechanism of strain aging, it does not predict the change in mechanical properties incurred during aging. There is also the challenge of obtaining sufficient data on the dislocation density.

As discussed above, plastic strain (i.e., dislocation generation) is an important variable in strain aging. An artificially applied strain (to a skelp material) can be used to quantify the effect of this variable on strain aging (see Table I). Conversely, for pipe material, the strain history (e.g., magnitude, direction, strain reversals, etc.,) at each point around the pipe circumference is complicated and in many instances is not known exactly. Given the potential importance of plastic strain on the aging phenomenon, a review of strain history incurred during pipe forming will be undertaken.

Regardless of the pipe making operation used (e.g., ERW, UOE and spiral), different plastic deformation histories can arise from the cold forming of a flat skelp into a round pipe. In the most simplistic case, the inner diameter (ID) or outer diameter (OD) of the pipe will experience the largest strain while the centre line (CL or neutral axis) will experience the smallest or negligible plastic strain. However, the magnitude and complexity (e.g., compression and/or tension and/or reversals) of the plastic strain depends on both the pipe diameter and the exact forming conditions [2-7]. The strain history can affect the initial mechanical properties of the pipe [17-21]. In addition, the Bauschinger effect can occur during pipe forming [17], which may reduce the dislocation density via dislocation annihilation on reverse loading.

Thus, to best quantify the effect of actual strain history, incurred during forming, on aging behaviour, it is necessary to obtain tensile samples directly from a formed and non-aged (i.e., uncoated) pipe. In this study, the aging behaviour of three (3) uncoated UOE pipes is analyzed. As all three pipes are produced by the same process, and are of similar wall thicknesses, it is assumed that the strain history incurred in each pipe is similar. The main differences between the three UOE pipes is the microstructure.

2.3 *Box Behnken Statistical Design*

Response surface (RS) analysis is a statistical technique for developing, improving and optimizing a process by the design of experiments [22]. In particular, RS is useful for modelling the quadratic response of a set of continuous variables and/or the interactions between variables. The Box-Behnken Design (BBD) is an RS technique used to "fit" an empirical second order (quadratic) polynomial equation to data from a reduced number of tests. A second order response surface model would have the following form.

$$Y = \beta_o + \sum_{i=1}^{n} \beta_i \cdot x_i + \sum_{i=1}^{n} \beta_{ii} \cdot x_i^2 + \sum_{i=1}^{n} \sum_{j<i}^{n} \beta_{ij} \cdot x_i \cdot x_j \qquad (2)$$

where Y is the dependent variable of interest (e.g., Δ(Y/TS)), x_i represents the independent variables (e.g., temperature) and β_o, β_i, β_{ii} and β_{ij} are fitting constants.

BBD was used to study the effect of four (4) independent variables; temperature (T), time (t), position through the thickness (Pos) and the C/Nb ratio on Δ(Y/TS). The statistical software Minitab 17 was used to generate the test matrices for the BBD and for analysis and generation of the response surfaces and models.

3.0 Experimental

This section will outline the dimensions and composition of the UOE pipe steel analysed, a brief description of the tensile testing, the microstructure analysis conducted and the BBD parameters and levels.

3.1 Steel Composition

Three (3) different UOE pipe steels, (labeled A, B and C) were investigated in this work. Due to the proprietary nature of microalloyed steel production, the thermomechanical controlled processing (TMCP) processing history of each steel is not available and only selected compositions are provided. The UOE pipe dimensions, the nominal levels of Mn, N and Ti and the nominal C/Nb ratio, for each steel are shown in Table 2. The C/Nb ratio was considered as a variable as this ratio may have an effect on the amount of carbon remaining in solid solution and/or on the microstructure resulting from TMCP. The nominal levels for Mn, N and Ti for all three steels are very similar, while the C/Nb ratio varies significantly - from 0.6 in A to 1.2 in B to 1.8 in C.

Table 2 Nominal UOE pipe steel specifications

Steel	Diameter /mm	Wall Thickness /mm	Mn/wt%	N/ppm	Ti /wt%	C/Nb ratio
A	914	19.1	1.60	40	0.014	0.6
B	914	19	1.65	40	0.013	1.2
C	914	20.4	1.59	<40	0.017	1.8

3.2 Tensile testing

Longitudinal tensile tests samples were extracted from two locations on the UOE pipes; 90° relative to the weld and 180° relative to the weld, as shown in Figure 1a. Three (3) rectangular tensile samples were machined from positions near the inner ID, CL and OD, as shown in Figure 1b. The thickness midpoint of each OD and ID tensile sample corresponds to a distance of 7.5 mm above (+) and below (-) the CL, respectively. Aging was undertaken using a salt bath set at a temperature of either 175, 215 or 255°C. Test samples were instrumented with thermocouples to confirm the temperature. Tensile testing was conducted as per ASTM Standard E8/E8M-13a using an Instron universal testing machine with an initial crosshead speed of 1.56 mm/min. Elongation measurements were obtained from an extensometer.

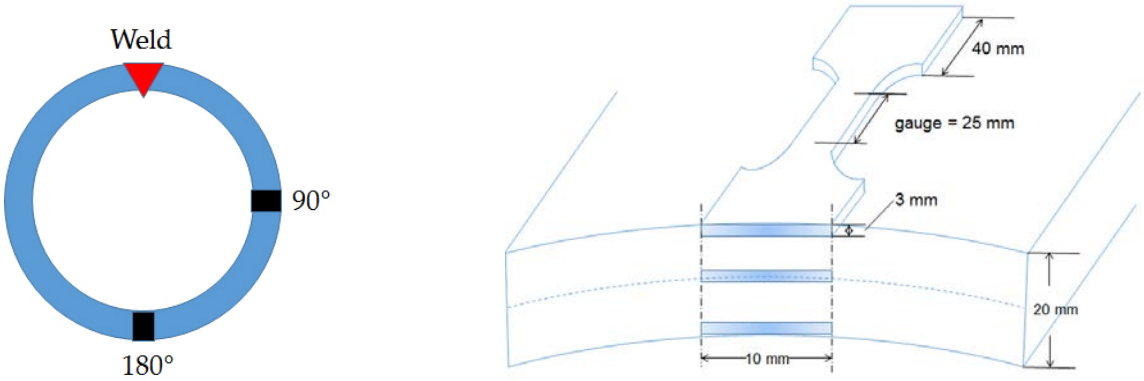

1 Tensile sample location: a) relative to the weld; b) through the wall thickness

3.3 Microstructure analysis

Metallographic samples of each steel (as-received pipe) from each of the through thickness positions (ID, CL and OD) were prepared from both the 90° and 180° locations. Optical microscopy (OM), scanning electron microscopy (SEM) and EBSD [23] were used to examine the microstructure. Qualitative assessment of the microstructure and quantitative analysis of grain size and phase percentage were undertaken using ASTM Standards E112-13 and E562-11, respectively. Grain size was measured using the linear intercept method (ASTM E112-13) from the OM and by the map method for EBSD. The volume percentage of each microconstituent for each steel was obtained from area analysis (using Image J software) of the OM microstructure images.

3.4 Box-Behnken Design: Parameters and Levels

The BBD methodology used in this work requires three (3) levels of the independent variables. The levels for each variable are designated by a -1, 0 or 1, which corresponds to the actual variable value as shown in Table 3. The variables examined include aging temperature (T), time at temperature (t), the C/Nb ratio (C/Nb) of each steel and position through the thickness (Pos), where -7.5 mm corresponds to the ID position, 0 mm to the centreline and +7.5 mm corresponds to the OD position. The values of temperature and time shown in Table 3 were selected to encompass the value of these parameters experienced in a pipe coating operation.

Table 3 Strain aging parameters and levels for BBD

Parameter	Levels		
	-1	0	1
Temperature/°C	175	215	255
Time/min	5	15	25
Position/mm	-7.5	0	+7.5
C/Nb	0.6	1.2	1.8

3.5 Additional Aged Tensile Samples

Additional tensile samples (not used in the BBD), from both the 90° and 180° locations, were aged under the same conditions as the independent variables shown in Table 3. The additional tensile samples from the 90° location were used as an independent verification of the response surfaces models generated from the BBD. The additional tensile samples obtained from the 180° location were used to assess the whether the strain aging model derived at the 90° location was valid at the 180° location.

4.0 RESULTS

The tensile test results and microstructure analysis (OM and EBSD) of the as-received steel will be presented, followed by the tensile test results from the strain aging tests. The results from the tensile tests will then be used in the BBD statistical and response surface analysis.

4.1 As-received Longitudinal Tensile Curves

The longitudinal (L) tensile curves for the as-received (AR) steels, taken from the 90° location (A1, B1 and C1) and CL position, are shown in Figure 2. Included in the figure is the 0.5% strain used to determine the yield stress for each steel. Steels A and B exhibit very similar tensile behaviour, while Steel C exhibits slightly different work hardening behaviour at low strain values. This difference is attributed to microstructural differences between the steels (to be discussed later).

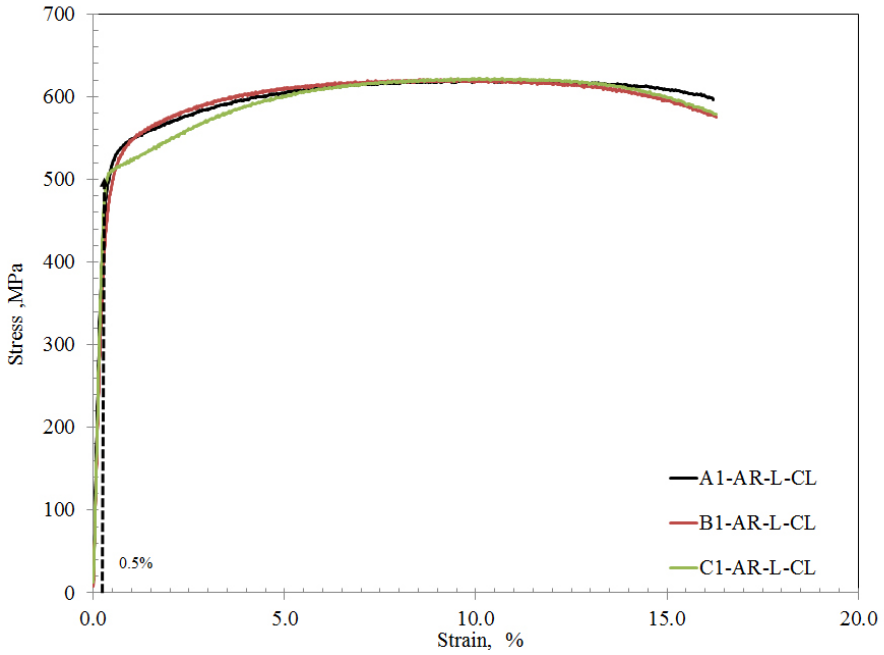

2 Longitudinal stress-strain curves for as-received pipe from the 90° location and CL position for Steel A, Steel B and Steel C.

Table 4 summarizes the longitudinal yield stress (σ_y), UTS and the yield strength to tensile strength ratio ((Y/TS)) for the as-received steels at both the 90° and 180° locations. The longitudinal properties of the as-received samples for Steel A and B are relatively uniform across the wall thickness and with respect to location relative to the weld, while Steel C exhibits different tensile behaviour between the CL (e.g., σ_y = 509 MPa) and the ID and OD positions (e.g., σ_{yID} = 577 MPa and σ_{yID} = 592 MPa).

Table 4 Summary of as-received tensile test results

Steel	Position	Location	σ_y/MPa	UTS/MPa	(Y/TS)
A	ID	90	525.5	601.3	0.87
A	CL	90	517.8	619.8	0.85
A	OD	90	528.7	601.6	0.88
A	ID	180	551.7	621.4	0.89
A	CL	180	529.7	619.3	0.86
A	OD	180	525.9	609.9	0.86
B	ID	90	499.0	596.9	0.84
B	CL	90	497.3	620.8	0.80
B	OD	90	488.5	598.3	0.82
B	ID	180	514.4	619	0.83
B	CL	180	500.8	622.7	0.80
B	OD	180	513.8	610.2	0.84
C	ID	90	577.0	647.9	0.89
C	CL	90	509.3	621.9	0.82
C	OD	90	592.1	666.5	0.89
C	ID	90	579.2	646.2	0.90
C	CL	90	513.5	619.1	0.83
C	OD	90	587.4	656.8	0.89
C	ID	90	563.8	648.4	0.87
C	CL	90	510.5	617.5	0.83
C	OD	90	573.9	654.9	0.88
C	ID	180	573.9	654.9	0.88
C	CL	180	510.5	617.5	0.83
C	OD	180	563.8	648.4	0.87

4.2 Microstructure Analysis

The as-received microstructures of Steel A, B and C at the ID, CL and OD positions were analyzed using OM, SEM and EBSD. The OM grain size was determined by counting the number of grain intersections with a circle of known size placed on the OM image. The volume percentage of each micro constituent in an OM image was obtained using ImageJ software.

The as-received microstructures for all three steels at the ID, CL and OD positions for the 90° location are shown in Figure 3. The microstructure of Steel A consists of needle shaped acicular ferrite (AF in Figure 3), polygonal ferrite (PF in Figure 3) and a small amount of pearlite (P in Figure 3). Steel B consists of acicular ferrite and ferrite. The Steel C microstructure consists of acicular ferrite, ferrite and extensive amounts of pearlite. SEM images for pearlite P in Steel C are shown in Figure 4. Qualitatively, the microstructure for Steel C is less uniform across the wall thickness (relative to Steel A and B) and exhibits a larger grain size at the CL versus either the OD or ID positons. Quantitative microscopy (discussed in the next section) confirmed this observation. The through wall thickness microstructures at the 180° location, for all three steels, are similar to those shown in Figure 3 at the 90° location.

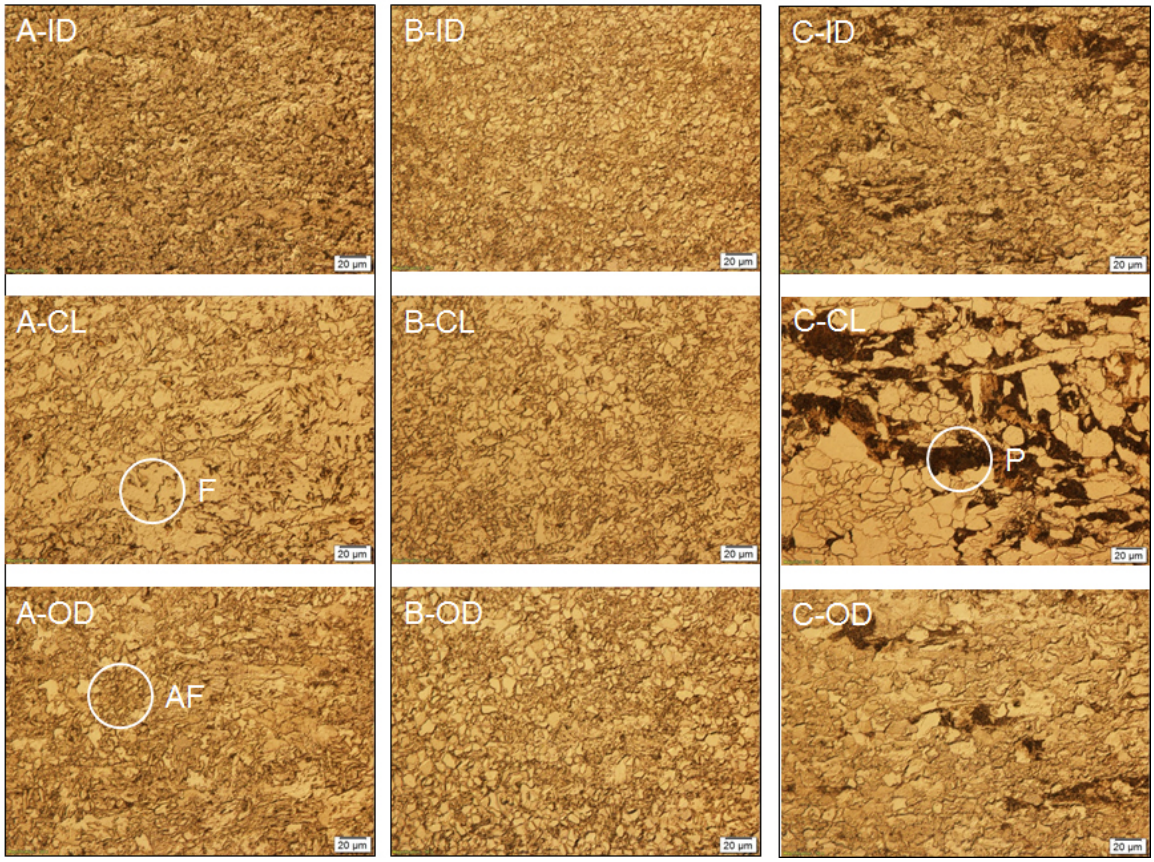

3 Microstructures for Steels A, B and C at the ID, CL and OD locations.

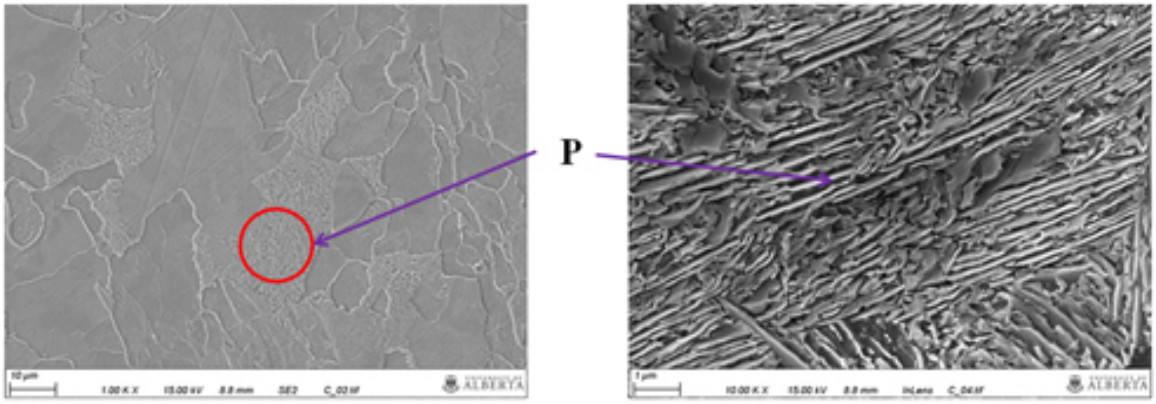

4 SEM secondary electron (SE) images for Steel C at the CL position.

The measured grain size and volume percentage of each microconstituent for all three steels at the ID, CL and OD locations are summarized in Table 5. Steel C has both a larger grain size (e.g., 16.4 μm at the CL) and a higher volume percentage of pearlite (e.g., 22% at the CL) than either Steel A or B. These differences are observed qualitatively in Figure 3. The combined effect of a variation in grain size (d) and the

amount of pearlite for Steel C at the ID, CL and OD locations may account for the variation in through thickness mechanical properties in the as-received tensile samples (Table 4). The grain size and volume percentages of each microconstituent measured at the 180° location are consistent with those measured in Table 5 (i.e., at the 90° location).

Table 5 Measured average grain size and volume percentage of microconstituents for the as-received steels at the 90° location

		Volume Percentage*/% (S.D.#/%)		
Steel	d*/μm (S.D./μm)	AF	PF	P
ID				
A	8.3 (0.5)	58.7 (1.2)	34.8 (2.6)	6.5 (2.0)
B	5.8 (0.5)	63.7 (4.2)	36.3 (4.2)	0
C	9.8 (0.48)	66.8 (3.7)	20.9 (3.5)	12.4 (1.5)
CL				
A	7.9 (0.3)	54.4 (5.3)	43.6 (0.4)	2.0 (0.4)
B	7.0 (0.5)	40.4 (2.7)	59.6 (2.7)	0
C	16.4 (0.9)	0	77.9 (3.4)	22.1 (3.4)
OD				
A	7.6 (0.6)	63.4 (6.1)	35.0 (5.6)	1.7 (0.8)
B	6.7 (0.3)	59.1 (4.1)	40.9 (4.1)	0
C	10.7 (0.5)	59.5 (2.5)	31.0 (2.5)	9.5 (1.9)

* Five (5) independent images examined

S.D. is the standard deviation

EBSD maps for Steel A, B and C at different through thickness positions are shown in Figure 5. The average grain size measured using the EBSD post-processing software CHANNEL5 is summarized in Table 6. The EBSD grain size is based on a misorientation angle of >15° and the conversion of the area of the grain into an equivalent diameter for a circle that encompasses an equal area. As with the OM

analysis, the largest grain size is measured for Steel C at the centreline. In addition, the trends in grain size values measured with EBSD (Table 6) are similar to the OM measurements (Table 5) in that the largest grain size is measured for Steel C at the centreline (EBSD = 10.4 µm vs. OM = 16.4 µm) and the surface grain sizes are smaller than the centreline grain sizes (except for B-ID). However, the standard deviations (S.D.) in the grain size measurements is larger than for OM.

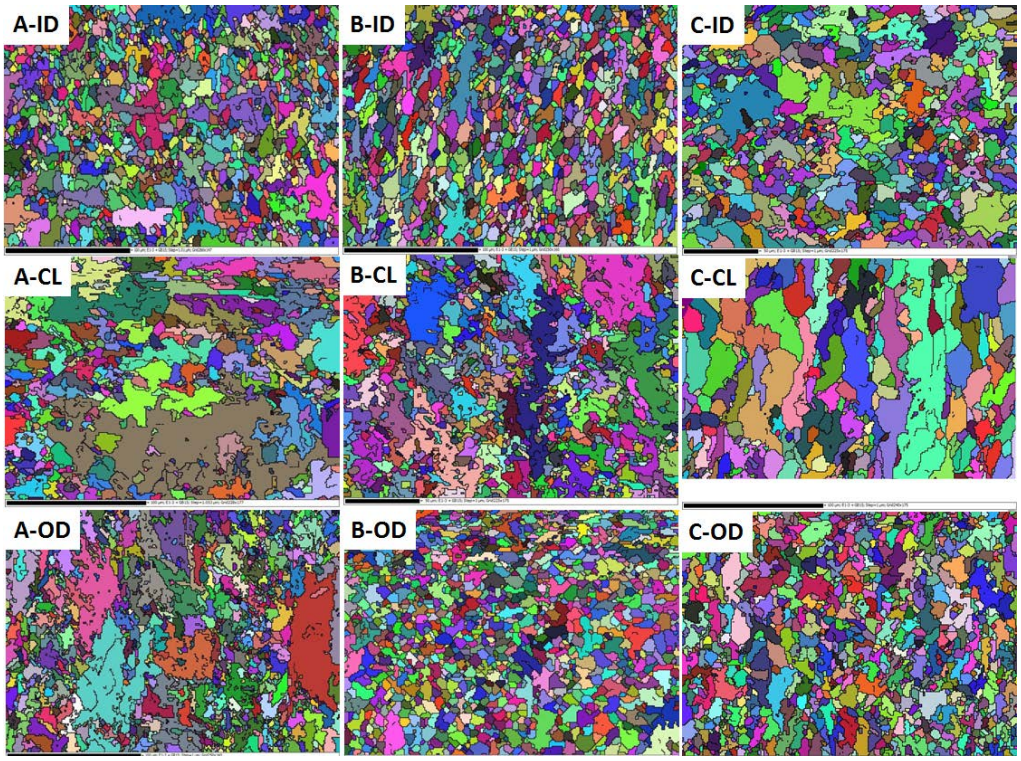

5 EBSD maps for Steel A, B and C (90°) at the ID, CL and OD positions.

Table 6 Average grain size of Steel A, B and C (90°) using EBSD

	ID	CL	OD
Steel	d/μm (S.D./μm)		
A	6.5 (3.0)	8.2 (5.2)	6.7 (4.4)
B	6.7 (2.9)	6.5 (3.4)	6.2 (2.4)
C	7.3 (4.1)	10.4 (6.9)	6.7 (3.1)

4.2 Tensile Test Results

The (Y/TS) values for the longitudinal samples, from the aged steels, used in the BBD are presented in this section. This is followed by a detailed examination of the BBD statistical analysis of the Δ(Y/TS) and its relation to the aging parameters.

4.2.1 (Y/TS) vs. Yield Strength

The relationship between the longitudinal (Y/TS) ratio and yield strength (0.5% offset) measured for all samples tensile tested, including the as-received and aged samples at both the 90° and 180°, is shown in Figure 6. (Y/TS) ratio increases as the yield strength (σ_y) increases. The as-received tensile samples exhibited a (Y/TS) ratio < 0.90 and a maximum σ_y of 592 MPa. In comparison, the aged samples showed a maximum (Y/TS) ratio of 0.95 and a maximum σ_y of 629 MPa. Although Figure 6 shows the relationship between (Y/TS) and σ_y, it does not illustrate how the (Y/TS) value changes as a function of microstructure, position and aging temperature and time. The BBD design discussed in subsequent sections will attempt to elucidate these relationships.

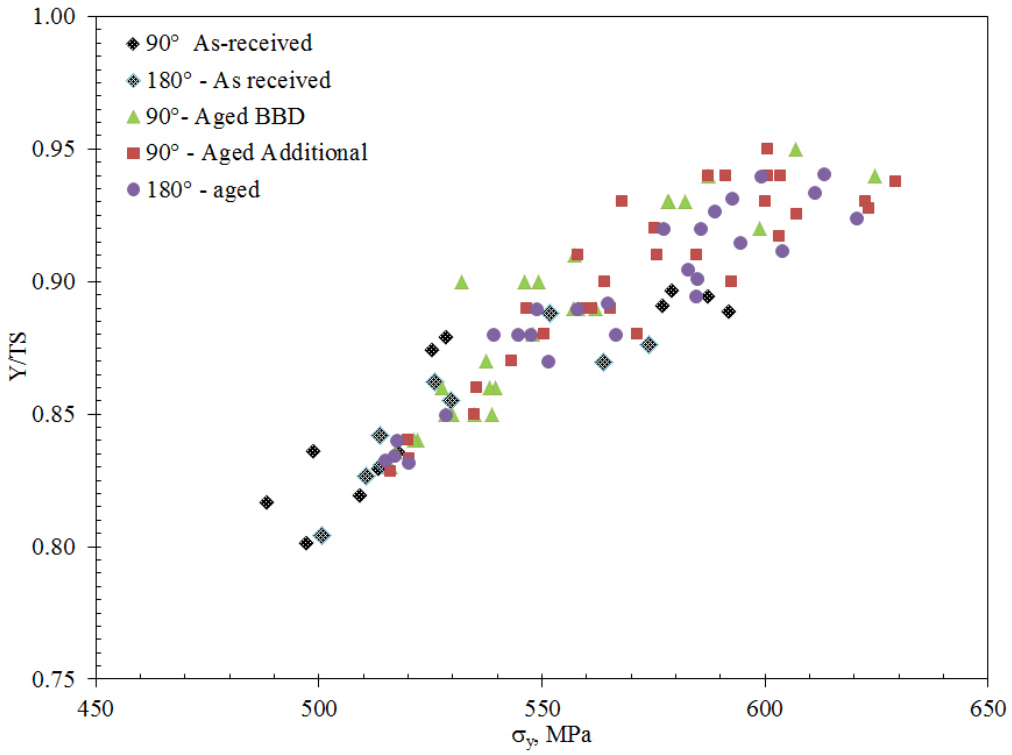

6 Measured (Y/TS) ratio as a function of yield strength for as-received and aged samples at both the 90° and 180° positions for Steels A, B and C.

4.2.2 Δ(Y/TS) at 90°

Table 7 summarizes the 27 tests undertaken in the BBD including the variable levels presented in Table 3. Also included in Table 7 are the measured changes in yield stress ($\Delta\sigma_y$), tensile strength (ΔUTS) and the yield strength to tensile strength ratio (Δ(Y/TS)) as a result of each aging treatment. Each property change is determined as the difference in the value for the aged sample minus the value for the as-received steel (Table 4). In general, the $\Delta\sigma_y$ changes to a greater extent than ΔUTS during strain aging. As an example, $\Delta\sigma_{yTest18}$ = 118.3 MPa versus ΔUTS_{Test18} = 39.2 MPa. This trend is not surprising given that the mechanism of strain aging entails the "pinning" of dislocations, which will have a greater effect on yield strength than on tensile strength.

Table 7 BBD Test Matrix and Measured Changes in Properties

Test	Temp	Time	Position	C/Nb	$\Delta\sigma_y$ /MPa	ΔUTS /MPa	Δ(Y/TS)
1	-1	-1	0	0	30.2	-8.2	0.060
2	1	-1	0	0	42.3	8.4	0.057
3	-1	1	0	0	35.0	0.0	0.056
4	1	1	0	0	41.6	10.1	0.053
5	0	0	-1	-1	58.7	24.1	0.083
6	0	0	1	-1	56.5	21.2	0.054
7	0	0	-1	1	32.6	5.7	0.045
8	0	0	1	1	21.8	4.1	0.030
9	-1	0	0	-1	19.7	-1.5	0.034
10	1	0	0	-1	39.3	3.7	0.025
11	-1	0	0	1	7.2	1.1	0.010
12	1	0	0	1	13.0	-0.2	0.021
13	0	-1	-1	0	73.5	34.4	0.072
14	0	1	-1	0	89.9	24.0	0.113
15	0	-1	1	0	47.2	9.6	0.065
16	0	1	1	0	50.3	14.7	0.062
17	-1	0	-1	0	68.8	11.6	0.097
18	1	0	-1	0	118.3	39.2	0.135
19	-1	0	1	0	32.9	-3.4	0.060
20	1	0	1	0	79.1	22.9	0.097
21	0	-1	0	-1	30.2	4.2	0.010
22	0	1	0	-1	40.3	8.1	0.020
23	0	-1	0	1	8.2	0.0	0.013
24	0	1	0	1	12.4	-1.6	0.022
25	0	0	0	0	37.5	10.7	0.057
26	0	0	0	0	40.9	6.7	0.044
27	0	0	0	0	31.1	4.4	0.050

4.2.3 Δ((Y/TS)) vs. ΔUEL

As discussed in the Introduction, the magnitude of the (Y/TS) ratio is a measure of the strain capacity of the steel (i.e., uniform elongation (UEL)). Figure 7 plots the change in Δ(Y/TS) versus ΔUEL for all the aged samples at the 90°C location. As aging of the steel may result in a reoccurrence of Luders yielding, the value for the change in UEL (*ΔUEL*) is calculated using:

$$\Delta UEL = \left(\varepsilon_{UTS} - \varepsilon_{Lud}\right)_{aged} - \left(\varepsilon_{UTS}\right)_{AR} \tag{3}$$

where ε_{UTS} is the strain measured at the tensile strength for either the aged or as-received (AR) samples and ε_{Lud} is Luder's strain for the aged samples. The trend observed in Figure 7 is that the larger the increase (i.e., positive) in Δ(Y/TS), the greater the reduction (i.e., negative) in the strain capacity (ΔUEL*)* of the steel.

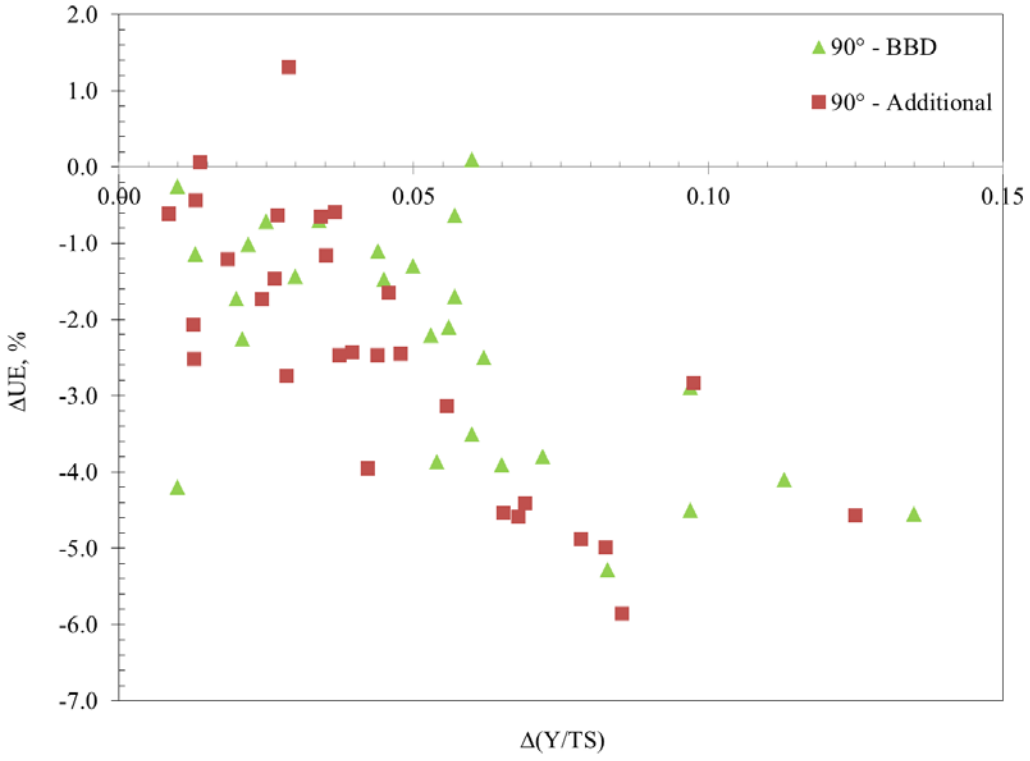

7 Measured ΔUEL versus Δ((Y/TS)) for all aged samples at the 90° position for Steels A, B and C.

4.2.4 Analysis of Δ((Y/TS)) – ANOVA Table

Using the Δ(Y/TS) and the temperature, time, position and C/Nb ratio values shown in Table 7, and the statistical software Minitab 17, analysis of variance (ANOVA) tables, quadratic equations and response surfaces were generated for the effect of strain aging on Δ(Y/TS). The reduced ANOVA data for the effect of temperature, time, position and C/Nb ratio on Δ(Y/TS) is shown in Table 8 and includes the degree of freedom (DF), sum of squares (SS) and the F-statistic (F-value) for the significant variable,. Only the variables, combination of variables and/or squared terms with a p-value <0.05 (indicates less than a 5% probability that the effect of the variable is due to noise) were deemed significant and are included in the reduced ANOVA table and subsequent response surface models. The significant variables for Δ((Y/TS)) are Pos, C/Nb, Pos^2 and C/Nb^2. A p-value of <0.001 indicates that there is a high degree of statistical correlation between the variable and Δ((Y/TS)).

The p-value for temperature was 0.140, which represents a significant greater probability of effecting Δ((Y/TS)) than random chance, but did not fall within the statistically significance level ($p < 0.05$) used as a criteria in this work. As such, temperature was excluded from subsequent analysis. Time (t) exhibited a p-value of 0.72 and did not have a statistically significant effect on Δ((Y/TS)) for the test conditions examined in this work. The relatively low statistical significance of temperature, and to a much greater degree time, is somewhat unexpected given the mechanism of strain aging requires the diffusion of carbon which is both temperature and time dependent.

Analysis of the effect of time and temperature on the change in yield strength (ΔY) shows that ΔY increases with both increasing temperature and time. This behaviour is consistent with previous strain aging studies. However, the magnitude of their singular or combined effects on ΔY (for the conditions studied in this work) is relatively small in comparison to the effects of steel type and through thickness wall positon. Thus, the effect of time and temperature on Δ((Y/TS) is “overshadowed” by these other variables, and hence, their relatively low statistical significance in the Box-Behnken analysis.

Table 8 Reduced ANOVA Data for Δ((Y/TS))

Term	DF	SS	F-value	p-value
Model	4	0.0218	28.8	<0.001
Pos	1	0.0026	13.8	<0.001
C/Nb	1	0.0067	35.1	<0.001
Pos^2	1	0.0073	38.4	<0.001
$(C/Nb)^2$	1	0.0076	40.3	<0.001
Residual	22	0.0041		
Lack of Fit	20	0.00408	4.8	0.19
R^2	0.84			

4.2.5 Δ(Y/TS) *Aging Response - Model*

The uncoded response surface model for predicting the change in Δ(Y/TS) is as follows:

$$\Delta(Y/TS) = -0.0701 - 0.00197 \cdot Pos + 0.2185 \cdot \left(\frac{C}{Nb}\right) + 0.000599 \cdot Pos^2 - 0.0959 \cdot \left(\frac{C}{Nb}\right)^2 \quad (5)$$

To assess the validity of the model, a parity plot comparing the measured (Table 7) Δ(Y/TS) values and predicted values (Equation 5) is shown in Figure 8. The measured and modelled data match each other relatively well. The smallest Δ(Y/TS) value was predicted and measured for Steel C at the CL. Conversely, the largest Δ(Y/TS) value was associated with Steel B at the ID location. The measured Δ(Y/TS) values and predicted values (Equation 5) for additional aging data (i.e., data not used in the BBD formulation) at the 90° location are shown in Figure 9. Except for one (1) point (Steel B – ID with Δ(Y/TS) = 0.013), the model fits the data well confirming the veracity of the model shown in Equation (5).

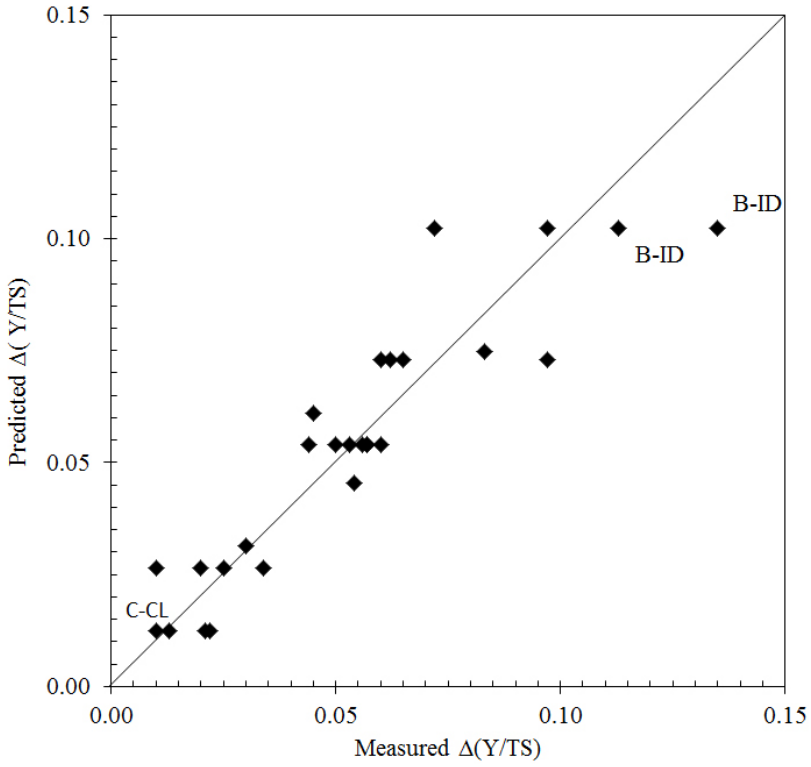

8 Parity plot for Δ(Y/TS) at the 90° location using BBD data.

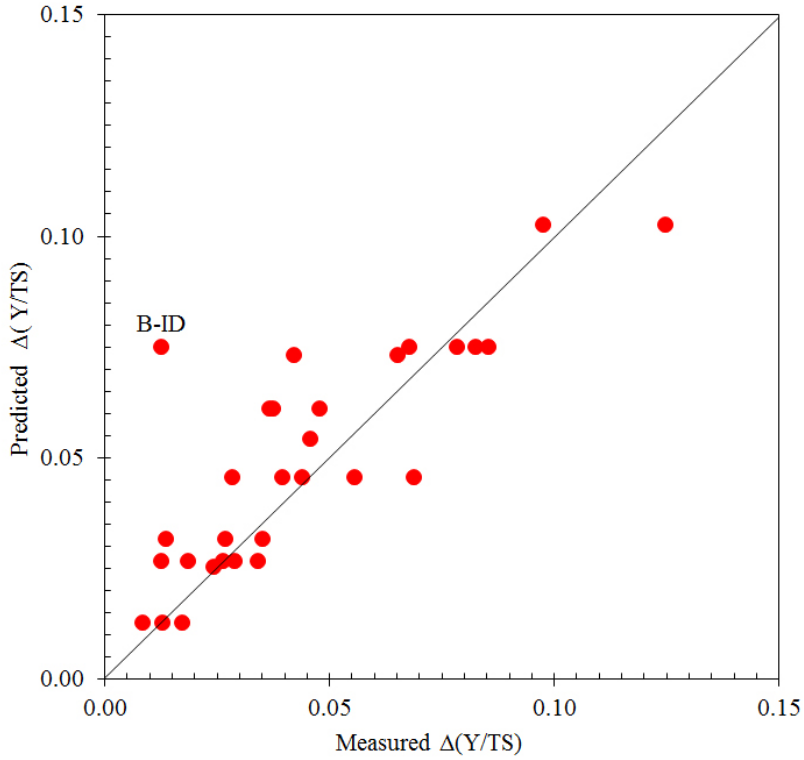

9 Parity plot for Δ(Y/TS) at the 90° location using the additional data.

4.2.6 Δ(Y/TS) Aging Response – Response Surfaces

The response surface plot for Δ(Y/TS) (based on Equation 5) as function of position (Pos) and C/Nb ratio is shown in Figure 10. The saddle shape of the aging response surface curve indicates the complexity of the effect of pipe through wall thickness position and steel type on the aging response of uncoated UOE pipe steel. The largest change in Δ(Y/TS) is related to the position through wall thickness, with the ID positon (Pos = -7.5 mm) exhibiting the largest change relative to the CL and OD positions. As will be discussed later, this difference may be attributed to both a difference in strain history (incurred during forming) and microstructural differences.

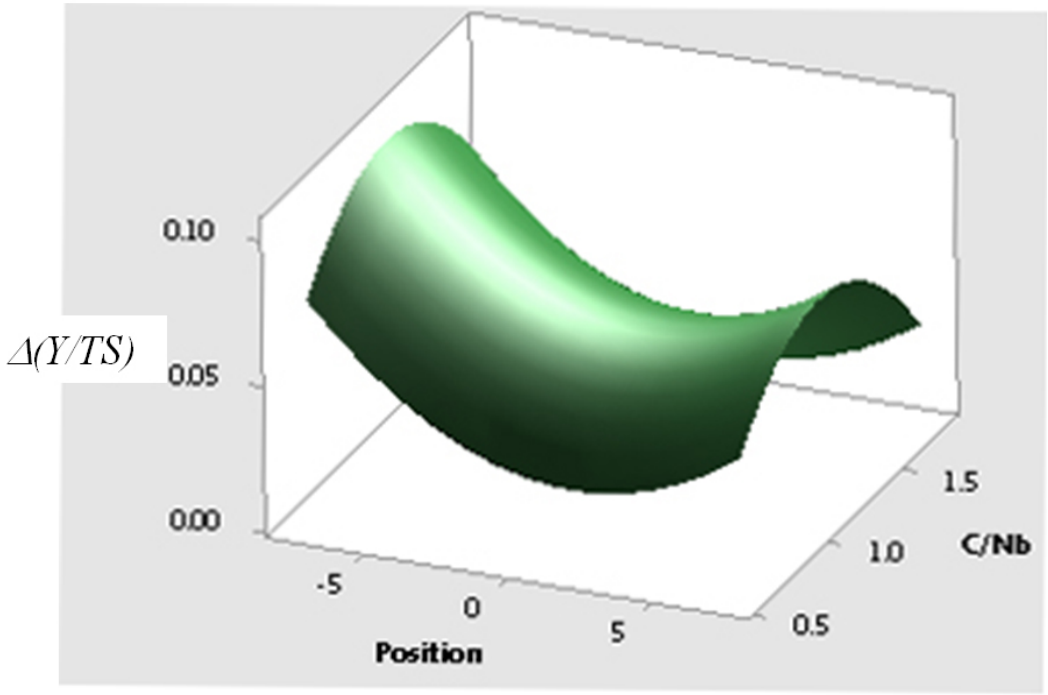

10 Response surface for Δ(Y/TS) generated using Equation 5.

4.2.7 Δ(Y/TS) Aging Response – Effect of Location

A comparison between Δ(Y/TS) measured at the 180° location and the predicted Δ(Y/TS) using Equation (5) is shown in Figure 11. Unlike Figures 8 and 9, there is significant difference between the measured data and the predicted values, particularly at the ID positions for Steel B. This data suggests that aging behaviour is different for the 90° and 180° locations for UOE pipe. This may be due to a difference in strain history between the two locations. The results also show that the microstructure for Steel B appears to be more susceptible to this strain history difference.

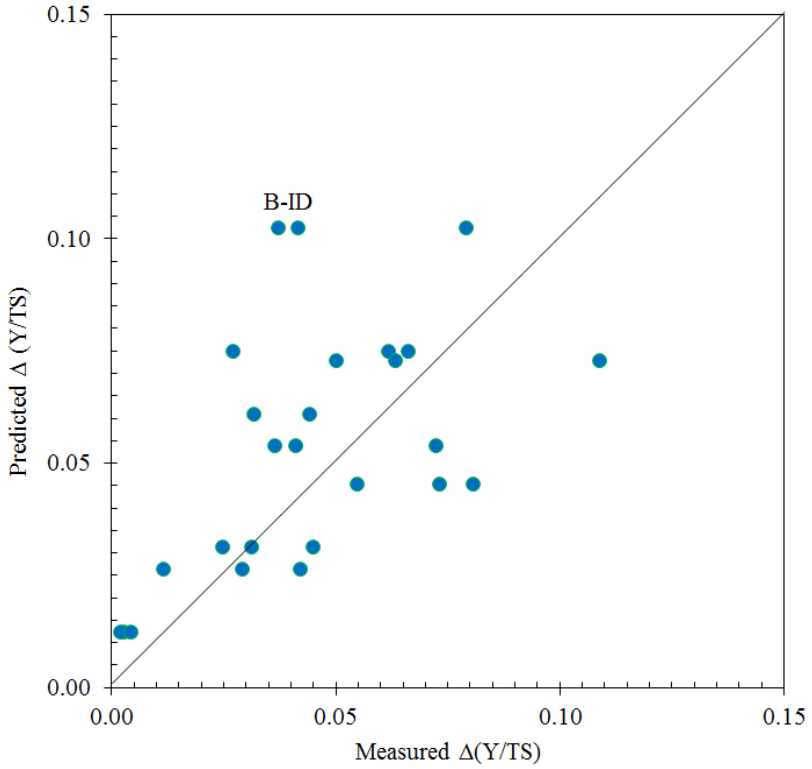

11 Parity plot for Δ(Y/TS) measured at the 180° location for all three steels aged at various time and temperatures and through thickness locations versus predicted values from Equation 5.

5.0 Discussion

The results from the Box-Behnken analysis indicate that both through wall thickness position (Pos) and the C/Nb ratio are statistically significant variables for Δ(Y/TS) during strain aging. For the aging conditions studied in this work, temperature to a certain extent and definitely time do not have a statistically significant effect on Δ(Y/TS). The Pos and the C/Nb ratio (i.e., steel type) are directly associated with varying steel microstructural phase percentage and grain size. In addition, the strain history incurred during forming of the pipe is different at the ID, CL and OD positions, which complicates assessment of the effect of Pos on strain aging behaviour.

5.1. Effect of Microstructure on Δ(Y/TS)

The effects of both C/Nb ratio (steel type) and Pos on Δ(Y/TS) are considered in terms of the microstructural features measured for each of the three steels, specifically the volume percentage of each phase and grain size across the pipe wall thickness.

5.1.1 Phase Volume Percentage

The volume percentages of acicular ferrite (AF) and polygonal ferrite (PF) for all three steels across the wall thickness are shown in Figure 12 and 13, respectively. Figure 12 shows that Steel A and Steel B exhibit significantly higher percentages of acicular ferrite (AF) (54% and 40% respectively) at the CL than Steel C (0%). In addition, Steel A exhibits the best uniformity across the thickness. In Figure 13, polygonal ferrite (PF) is the dominant phase at the CL for Steel C (78%). The higher level of AF observed at both the ID and OD is related to the higher cooling rate experienced (during TMCP) at these pipe through thickness locations.

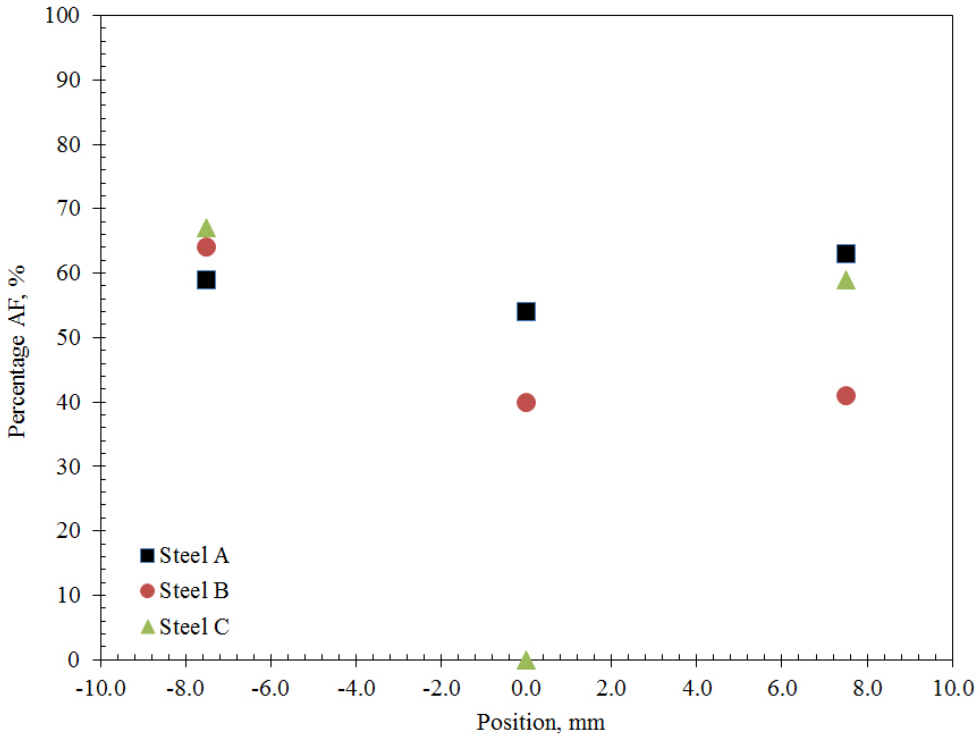

12 Measured volume percentage of acicular ferrite (AF) as a function of position through the pipe wall thickness.

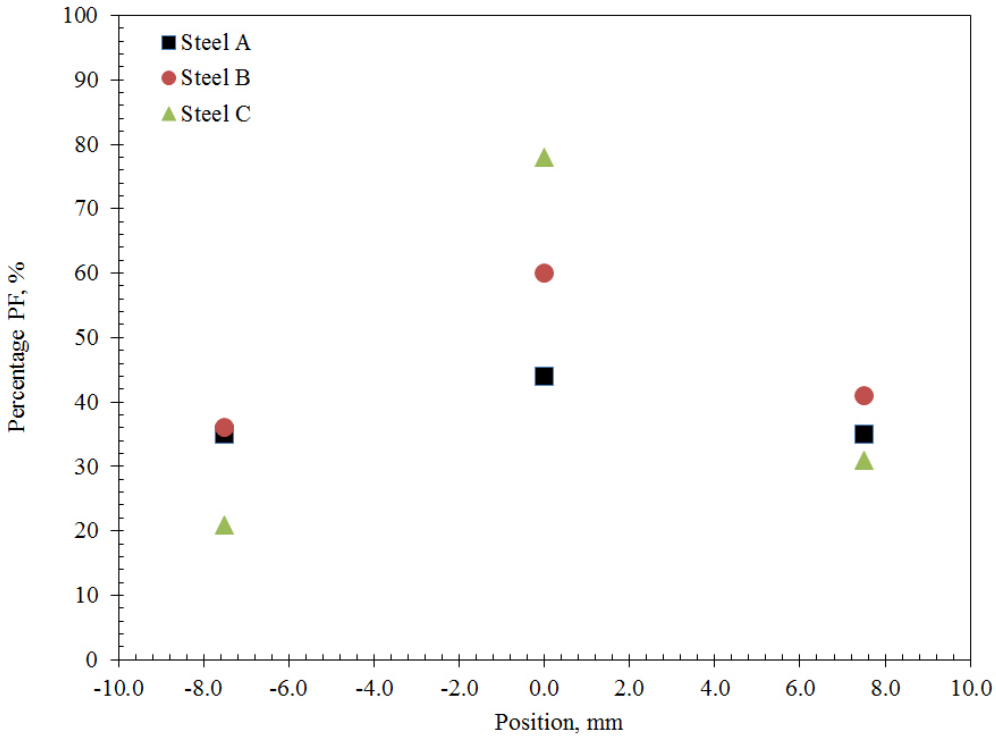

13 Measured volume percentage of polygonal ferrite (PF) as a function of position through the pipe wall thickness.

The presence of AF at the CL for Steel A and Steel B suggests an initial higher dislocation density in the steel microstructure vis-à-vis the predominantly polygonal ferritic (PF) observed for Steel C. As noted earlier, the as-received tensile curves for Steels A, B and C at the CL position (Figure 2) exhibited relatively similar UTS and UEL values but different initial work hardening behaviour. Both Steel A and Steel B had lower strain hardening coefficients than Steel C (0.116 for C vs. 0.104 and 0.096 for A and B respectively). This difference in the strain hardening coefficients suggests that the initial dislocation density in Steel C at the CL is lower than the dislocations densities for Steels A and B. Figure 14 plots the value of Δ(Y/TS) as a function of the percentage of AF. Although there is a trend towards a higher Δ(Y/TS) with increasing AF, the grain size also varies across the thickness. This effect is considered in the next section.

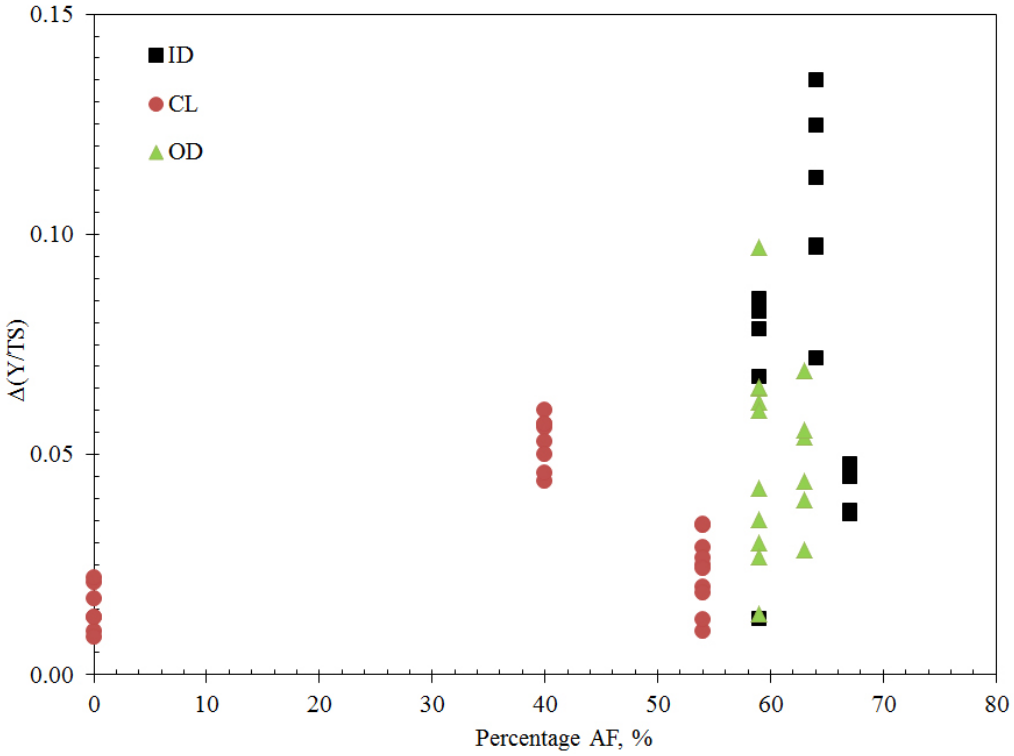

14 Measured Δ(Y/TS) at the 90° location versus percentage of acicular ferrite.

5.1.2 Effect of Grain Size

The OM grain size varies across the wall thickness of the pipe (Table 5) and for each steel. A similar trend is observed for the EBSD grain size data (Table 6); however, for the purpose of this section only the OM data will be considered due to its lower standard deviation. Grain size is known to affect the value of the yield stress via Hall-Petch strengthening, but its effect on strain aging is not clear. It is conceivable that a small grain size would influence the kinetics of strain aging by providing high diffusivity paths for carbon along the grain boundaries. However, as temperature and time were not statistically significant, it is possible that grain size has an influence on dislocation morphology. Narutani et al. [24] showed that dislocation density during plastic deformation of aluminum and copper varies inversely with grain size (1/d) (i.e., for a given plastic strain (e.g., encountered during pipe forming) the dislocation density after deformation will be higher for a material with a finer grain size). To account for the combined effect of acicular ferrite and grain size, a plot of Δ(Y/TS) as a function of the percentage of acicular ferrite divided by grain size for the ID, CL and OD positions (90° location) is shown in Figure 15. As grain size decreases and/or the amount of acicular ferrite increases, the change in Δ(Y/TS) increases indicating that the starting microstructure plays a role in the strain aging behaviour of a high strength pipe steel.

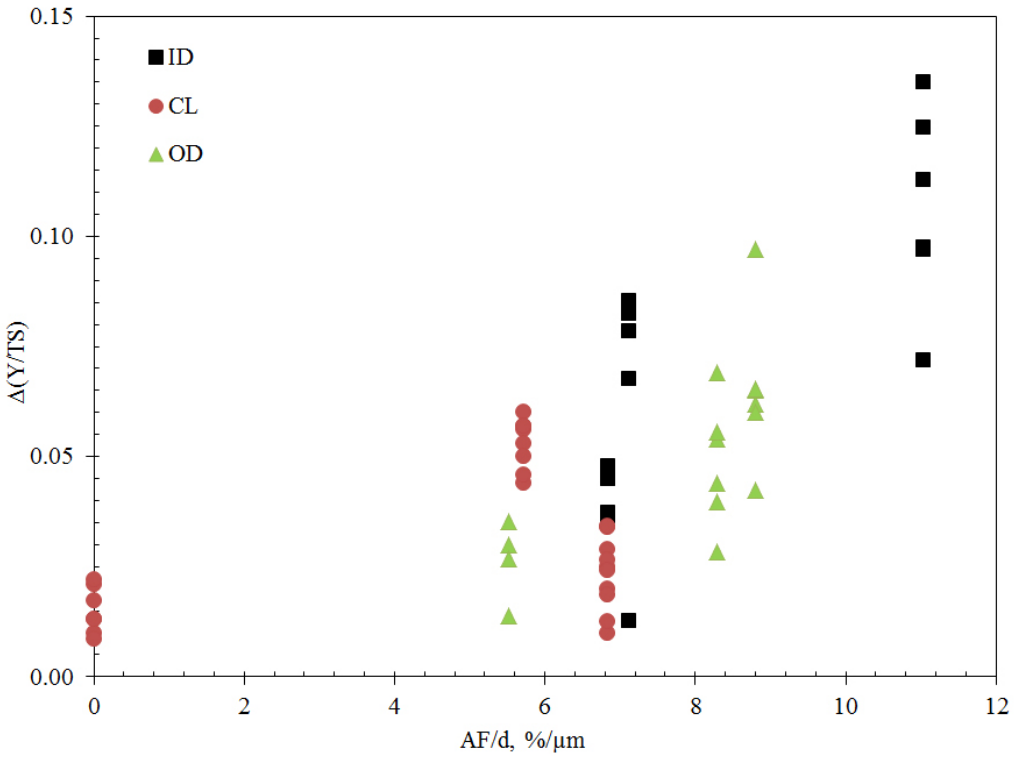

15 Plot of Δ(Y/TS) at the 90° location as a function of percentage of acicular ferrite (AF) divided by grain size.

5.2 Effect of Position on Δ(Y/TS)

In previous sections, it was shown (Figure 12) that the microstructure varies across the wall thickness and influences the response to aging of the steel. In addition, variations in strain history through the pipe wall thickness can occur during the forming process. Steel A exhibits a relatively uniform microstructure across the wall thickness (Table 5), both in terms of phase percentage and grain size; thus strain aging of this steel can be used as a measure of the effect of strain history on aging. Figure 16 plots the Δ(Y/TS) ratio for steel A as a function of wall thickness position after aging the steel at a constant aging temperature of 255°C. The ID position (Pos = -7.5) has a higher level of Δ(Y/TS) than the CL and to lesser extent the OD positions. The difference may be attributed to a difference in effective accumulated plastic strain (including possible dislocation annihilation due to the Bauschinger effect) during the forming process, where the lowest effective accumulated plastic strain is at the centreline.

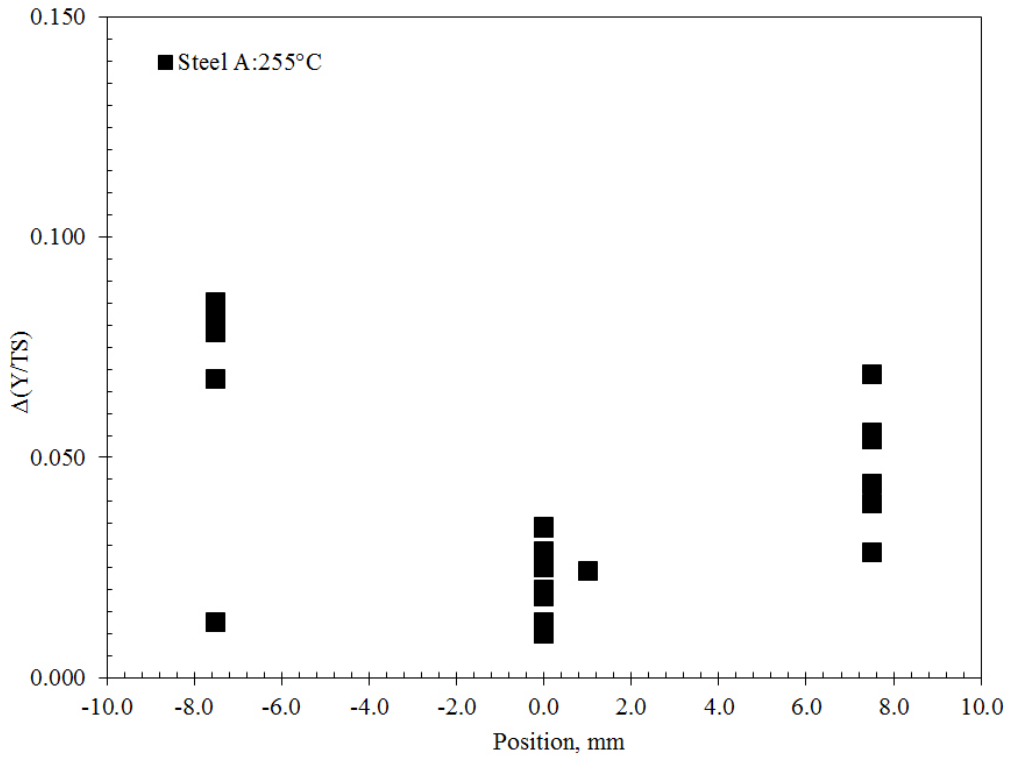

16 Plot of Δ(Y/TS) versus position for Steel A (255°C aging temperature).

6.0 Conclusions

The effect of temperature, time, C/Nb ratio (i.e., three different steels) and through wall thickness position on the longitudinal strain aging behaviour of X70 UOE pipe was studied. A Box-Behnken Statistical Design was undertaken to determine which of the proceeding variables (and/or combination of variables) had a statistically significant effect on the change in the yield strength to tensile strength ratio.

1] The significant strain aging variables affecting the change in longitudinal yield strength to tensile strength ratio (Δ(Y/TS)) of UOE X70 pipeline steel is the C/Nb ratio (via the steel microstructure) and position through the wall thickness of the pipe (i.e., outer diameter (OD), inner diameter (ID) and center line (CL) positions).

2] The magnitude of change in Δ(Y/TS) during aging increases with increasing amounts of acicular ferrite and with decreasing grain size. The former is attributed to a higher initial dislocation density.

3] The aging response of was observed to vary across the wall thickness with the centreline position showing the lowest change in Δ(Y/TS). The effect of through thickness position on Δ(Y/TS) is attributed to both a difference in microstructure at different through thickness positions and the possible variation in plastic strain through the thickness of the pipe that occurs during the UOE forming process.

4] Sample position relative to the weld had an effect on the Δ(Y/TS) ratio. The 180° pipe location exhibited a lower change in Δ(Y/TS) for similar aging temperature and times relative to the changes in Δ(Y/TS) at the 90° location. The difference is attributed to the difference in strain history at each location during the UOE forming process.

7.0 Acknowledgments

The authors would like to thank the Natural Sciences and Engineering Research Council (NSERC) of Canada, EVRAZ N.A., Enbridge, TransCanada Pipelines, Alliance Pipelines and UT Quality for financial assistance.

8.0 References

1. M. Katsumi and N. Yutaka, “Manufacturing Processes and Products of Steel Pipes and Tubes in JFE Steel”, JFE Technical Report, 7, 2006.
2. J.D. Baird, “The effects of strain-ageing due to interstitial solutes on the mechanical properties of metals”, Metallurgical Reviews, pp. 1-18, 1971.
3. F. Yang, Z. Sun and W. Zhang, “Effects of strain ageing on the microstructure of microalloyed steels”, Baosteel Tech. Res., 3(4), pp. 61-64, 2009.
4. H.S. Park, J.S. Kang, J.Y. Yoo and C.G. Park, “In-situ TEM and APT Analysis on the Dislocations Associated with Solute Carbons in Strain-Aged Low Carbon Pipeline Steels”, Mat. Sci. For., 654-656, pp. 122-125, 2010.
5. G.T. Van Rooyen, “The embrittlement of hardened, tempered low-alloy steel by strain aging”, J. S. Afr. INst. MNin. Metall., 86 (2), pp. 67-72, 1986.
6. G. Liang, X. Peng, E. Juan and Y. F. Cheng, “Strain Aging of X100 Steel in Service and the Enhanced Susceptibility of Pipelines to Stress Corrosion Cracking”, J. Mat. Eng, and Per., Aug, 2013.
7. S. Lou and D.O. Northwood, “Effect of Strain Aging on the Strength Coefficient and Strain-Hardening Exponent of Construction Grade Steel”, J. Mat. Eng. Perform., 3(3), pp. 344-349, 1994.
8. Q. Chi, L. Ji, P. Wang, Y. Li and L. Qi, “Effect of Cold Bending Process and Strain-Age of Properties of X80 Linepipe”, Conf. Proc. ICPPT 2012, Wuhan, China, pp. 1317-1327, 2012.
9. H, Shitamoto, M. Hamada, N. Takahashi and Y. Nishi, “Effect of thermal aging on the strain capacity of X80 SAW pipes”, Proc. 9th Int. Pipeline Conf., Calgary, IPC2012-90365, 2012.
10. X. Zhang, H. Gao, L. Ji and C. Zhuang, “Influence of Strain Aging on the Microstructure-Property of an X100 Pipeline steel”, Mat. Sci. Forum, 658, pp. 157-160, 2010.
11. T. Hara, Y. Terada, Y. Shinohara and H. Asahi, “Metallurgical design and development of high deformable X100 linepipe steels suitable for strain-based design”, Proc.7th Int. Pipeline Conf., Calgary,IPC2008-64234, 2008
12. W.Zhao, M.Chen, S. Chen and J. Qu, “Static strain aging behavior of an X100 pipeline steel”, Mat. Sci. Eng. A, 550, pp. 418-422, 2012.
13. E. Tsuru, and H. Asahi, “Collapse pressure prediction and measurement methodology of UOE pipe”, Int. J. Off. Polar Eng., 14(1), pp. 52-59, 2004.
14. F.H. Vitovec, “Strain Aging and Formability fo HSLA linepipe Steels”, J. Mat. Eng. Sys. Vol. 2, June, pp. 83-88, 1980..
15. P. McConnell and E.B. Hawbolt, “A Strain Age Study of Acicular Ferrite X-70 Pipeline Steels”, J. Mat Energy Sys., 1 (9), pp 25-31, 1979.

16. J.Z. Zhao, A.K. De and B.C. De Cooman, “Kinetics of Cottrell atmosphere formation during strain aging of ultra-low carbon steels”, Mat. Let, 44, pp. 374-378, 2000.

17. J.B. Wiskel, M. Rieder and H. Henein, “Kinematic Behaviour of Microalloyed Steels Under Complex Forming Conditions”, Can. Met. Quart., 43(1), pp. 125-136, 2004.

18. D. Uko, R. Sowerby and J.D. Embury, “Part 2 empirical analysis of influence of Bauschinger effect in pipe-forming operation”, Met. Tech., Sept, pp. 368-371, 1980.

19. S.S. Sohn, S,Y, Han, J. Bae, H.S. Kim and S. Lee, “Effects of microstructure and pipe forming strain on yield strength before and after spiral pipe forming of API X70 and X80 linepipe steel sheets”, Mat. Sci. Eng. A, A573, pp. 18–26, 2013.

20. D. N. Williams, “Interaction between the Bauschinger Effect and Strain Aging”, Met. Trans. A, pp. 1629-1631, 1980.

21. M.D. Richards, E.S. Drexler and J.R. Fekete, “Aging-induced anisotropy of mechanical properties in steel products: Implications for the measurement of engineering properties”, Mat. Sci. Eng. A, A529, pp. 184–191, 2011.

22. M. Thiyagu, L. Karunamoorthy and N. Arunkumar, “Experimental Studies in Machining Duplex Stainless Steel using Response Surface Methodology”, IJMME-IJENS, Vol. 14 (3), pp. 48-61, 2014.

23. J. Ma, M.A.Sc. Thesis, University of Alberta, Canada, 2016.

24. T. . Narutani and J. Takamura, "Grain-size strengthening in terms of dislocation density measured by resistivity," Acta Met. Mat., Vol. 39 (8), pp. 2037-2049, 1991.

Figure Captions

1 Tensile sample location: a) relative to the weld; b) through the wall thickness.

2 Longitudinal stress-strain curves for as-received pipe from the 90° location and CL position for Steel A, Steel B and Steel C.

3 Microstructures for Steels A, B and C at the ID, CL and OD locations.

4 SEM secondary electron (SE) images for Steel C at the CL position.

5 EBSD maps for Steel A, B and C (90°) at the ID, CL and OD positions.

6 Measured (Y/TS) ratio as a function of yield strength for as-received and aged samples at both the 90° and 180° positions for Steels A, B and C.

7 Measured ΔUEL versus Δ((Y/TS)) for all aged samples at the 90° position for Steels A, B and C.

8 Parity plot for Δ(Y/TS) at the 90° location using BBD data.

9 Parity plot for Δ(Y/TS) at the 90° location using the additional data.

10 Response surface for Δ(Y/TS) generated using Equation 5.

11 Parity plot for Δ(Y/TS) measured at the 180° location for all three steels aged at various time and temperatures and through thickness locations versus predicted values from Equation 5.

12 Measured volume percentage of acicular ferrite (AF) as a function of position through the pipe wall thickness.

13 Measured volume percentage of polygonal ferrite (PF) as a function of position through the pipe wall thickness.

14 Measured Δ(Y/TS) at the 90° location versus percentage of acicular ferrite.

15 Plot of Δ(Y/TS) at the 90° location as a function of percentage of acicular ferrite (AF) divided by grain size.

16 Plot of Δ(Y/TS) versus position for Steel A (255°C aging temperature).